

# ON THE BEHAVIOR OF UPWIND SCHEMES APPLIED TO COLD GAS HYPERSONIC FLOW SIMULATIONS OF INLET CONFIGURATIONS

**Farney Coutinho Moreira**

Instituto Tecnológico de Aeronáutica, CTA/ITA/PG-EEC, 12228-900, São José dos Campos, BRAZIL  
farney@ita.br

**João Luiz F. Azevedo**

Instituto de Aeronáutica e Espaço, CTA/IAE/ASE-N, 12228-904, São José dos Campos, BRAZIL  
azevedo@iae.cta.br

**Abstract.** *A comparison of five different spatial discretizations schemes is performed considering a typical high speed flow application. A fully explicit, 2nd-order accurate, 5-stage, Runge-Kutta time stepping scheme is used to perform the time march of the flow equations. The algorithms studied include a central difference-type scheme, and 1st- and 2nd-order van Leer and Liou flux-vector splitting schemes. The implementation uses a cell centered, face-based data structure. In order to enhance the quality of the results, mesh refinement routines were implemented in the code to adapt the original mesh. These routines are able to handle tetrahedra, hexahedra, triangular-base prisms and square-base pyramids. A sensor based on density gradients selects the elements to be refined. A full multigrid scheme is implemented to accelerate convergence to steady state. Grid levels are constructed through an agglomeration procedure. The application of interest is the cold gas flow through a typical hypersonic inlet. Results for different entrance Mach numbers are discussed in order to assess the comparative performance of the various spatial discretization schemes.*

**Keywords:** *CFD, Unstructured grids, Multigrid technique, Hypersonic flows, Upwind schemes*

## 1. Introduction

Upwind schemes take into account physical properties of the flow in the discretization process and they have the advantage of being naturally dissipative. Flux vector splitting methods introduce the information of the sign of the eigenvalues in the discretization process, and the flux terms are split and discretized according to the sign of the associated propagation speeds. Steger and Warming (1981) make use of the homogeneous property of the Euler equations and split the flux vectors into forward and backward contributions by splitting the eigenvalues of the Jacobian matrix into non-negative and non-positive groups. The split flux contributions are, then, spatially differenced according to one-sided upwind discretizations. However, these forward and backward fluxes are not differentiable when an eigenvalue changes sign, and this can produce oscillations at sonic points. In order to avoid these oscillations, van Leer (1982) defines a continuously spatially differenced flux vector splitting scheme that leads to smoother solutions at sonic points.

In the present work, the interface fluxes are calculated by five different algorithms, including a central difference-type scheme, and van Leer (1982) and Liou (1996) flux vector splitting schemes. In the central difference case, the interface fluxes are obtained from an average vector of conserved variables at the interface, which is calculated by straightforward arithmetic averages of the vector of conserved variables on both sides of the interface. For the first-order van Leer scheme, the interface fluxes are obtained by van Leer's formulas and they are constructed using the conserved properties for the  $i$ -th control volume and its neighbor across the given interface. The second order scheme considers a MUSCL approach (Anderson *et al.*, 1986), that is, the interface fluxes are formed using left and right states at the interface, which are linearly reconstructed by primitive variable extrapolation on each side of the interface. The extrapolation process is effected by a limiter in order to avoid the creation of new local extrema. The first- and second-order Liou schemes consider that the convective operator can be written as a sum of the convective and pressure terms (Liou, 1996). The second-order scheme also considers a MUSCL approach. Time march uses a fully explicit, 2nd-order accurate, five-stage Runge-Kutta time stepping scheme. Computations using a fine, unstructured mesh are compared to those obtained with an adaptive mesh procedure in order to assess the quality of the solutions calculated by the different schemes implemented and in order to analyze the mesh influence in the capture of the flow features of interest.

A 3-D inlet configuration which is representative of some proposed inlet geometries for a typical transatmospheric vehicle is considered. The inlet entrance conditions are varied from a freestream Mach number  $M_\infty = 4$  up to  $M_\infty = 12$  in order to test the schemes implemented for a wide range of possible inlet operating conditions. The fluid was treated as a perfect gas and, hence, no chemistry was taken into account. From a physical standpoint, the present simulations are typical of cold gas flows which are usually achieved in experimental facilities such as gun tunnels. This is certainly not representative of actual flight conditions in which dissociation and vibrational relaxation are important phenomena, especially for the higher Mach number cases. However, it is a necessary step in order to construct a robust code to deal with the complete environment encountered in actual flight.

## 2. Theoretical Formulation

A viscous formulation is available in the code, based on the Reynolds-averaged Navier-Stokes equations. The code handles turbulent flow problems through a suite of advanced one- and two-equation turbulence models. However, all calculations included in the present paper only considered inviscid computations, modeled by the Euler equations. Therefore, only this latter formulation is discussed here. The Euler equations can be written, considering the perfect gas assumption, as

$$\frac{\partial Q}{\partial t} + \frac{\partial E_e}{\partial x} + \frac{\partial F_e}{\partial y} + \frac{\partial G_e}{\partial z} = 0, \quad Q = [\rho \quad \rho u \quad \rho v \quad \rho w \quad e]^T. \quad (1)$$

where  $Q$  is the dimensionless vector of conserved variables,  $\rho$  is the fluid density,  $u$ ,  $v$  and  $w$  are the Cartesian velocity components and  $e$  is the fluid total energy per unit volume. In this work, all variables are non-dimensionalized according to Pulliam (1980). The  $E_e$ ,  $F_e$  and  $G_e$  terms are the dimensionless inviscid flux vectors, which can be written as

$$A_e = \begin{Bmatrix} \rho C \\ \rho u C + \delta_{kx} p \\ \rho v C + \delta_{ky} p \\ \rho w C + \delta_{kz} p \\ (e + p) C \end{Bmatrix}, \quad (2)$$

where  $A = E, F$  or  $G$ ,  $k = x, y$  or  $z$ , and  $C = u, v$  or  $w$ , respectively, and  $\delta_{ij}$  is the Kronecker delta.

## 3. Numerical Formulation

The forthcoming subsections briefly describe the finite-volume and temporal discretization of the governing equations.

### 3.1 Finite-Volume Discretization

The finite volume method (FVM) is used to obtain the solution of the governing equations. The formulation of the method is obtained by an integration of the flow equations in a finite volume. The application of Gauss theorem for each finite volume yields

$$\int_{V_i} \frac{\partial Q}{\partial t} dV + \int_{S_i} \vec{P}_e \cdot d\vec{S} = 0, \quad \vec{P}_e = E \vec{i}_x + F \vec{i}_y + G \vec{i}_z, \quad Q_i = \frac{1}{V_i} \int_{V_i} Q dV_i. \quad (3)$$

Here,  $d\vec{S}$  is the outward oriented normal area vector for the  $i$ -th control volume,  $\vec{i}_x$ ,  $\vec{i}_y$  and  $\vec{i}_z$  are the Cartesian unit vectors, and  $Q_i$  is the discrete value of the vector of conserved variables for the  $i$ -th control volume.

### 3.2 Time Integration

Time integration is performed using a Runge-Kutta type scheme, similar to the one proposed in Jameson *et al.* (1981). In the present work, a 2nd-order accurate, 5-stage Runge-Kutta scheme is used, which can be written as

$$\begin{aligned} Q_i^{(0)} &= Q_i^n, \\ Q_i^{(\ell)} &= Q_i^{(0)} - \frac{\alpha_\ell \Delta t_i}{V_i} (CO - DI)_i^{(\ell-1)}, \quad \ell = 1, \dots, 5, \\ Q_i^{n+1} &= Q_i^{(5)}. \end{aligned} \quad (4)$$

In the previous equations,  $CO_i$  and  $DI_i$  are, respectively, the convective operator and the artificial dissipation operator calculated for the  $i$ -th control volume. These operators are calculated according to the spatial discretization scheme. The  $\alpha_\ell$  coefficients are  $1/4$ ,  $1/6$ ,  $3/8$ ,  $1/2$  and  $1$  for  $\ell = 1, \dots, 5$ , respectively. The artificial dissipation operator is calculated only on the first and second stages. Furthermore, the artificial dissipation operator is computed only for the centered scheme. For the upwind schemes, the required artificial dissipation is intrinsically provided by the upwind discretization of the fluxes.

## 4. Spatial Discretization

### 4.1 Centered Scheme

The centered scheme used in this work for spatial discretization was proposed by Jameson *et al.* (1981). For this scheme, the convective operator is calculated as the sum of the inviscid fluxes on the faces of the  $i$ -th volume, which are computed as a function of the averaged vector of conserved properties at the face, i.e.,

$$CO_i = \sum_{k=1}^{nf} \vec{P}_e(Q_k) \cdot \vec{S}_k, \quad Q_k = \frac{1}{2} (Q_i + Q_m). \quad (5)$$

In this expression,  $Q_i$  and  $Q_m$  are the conserved properties in the volumes at each side of the  $k$ -th face and  $m$  indicates the neighbor of the  $i$ -th element.

## 4.2 First- and Second-Order van Leer Schemes

The convective operator,  $C(Q_i)$ , is defined for the van Leer flux vector splitting scheme (van Leer, 1982) by the expression

$$C(Q_i) = \sum_{k=1}^{nf} \left[ E_k \vec{i}_x + F_k \vec{i}_y + G_k \vec{i}_z \right] \cdot \vec{S}_k. \quad (6)$$

For the 2nd-order van Leer scheme, the interface fluxe  $E_k$ , is defined as

$$E_k = \begin{cases} E_e^+(Q_L) + E_e^-(Q_R) & \text{for } \vec{S}_k \cdot \vec{i}_x \geq 0 \\ E_e^-(Q_L) + E_e^+(Q_R) & \text{for } \vec{S}_k \cdot \vec{i}_x < 0 \end{cases} \quad (7)$$

Here,  $Q_L = Q(W_L)$  and  $Q_R = Q(W_R)$  are the left and right states at the  $k$ -th interface obtained by a linear, MUSCL extrapolation process (Farney and Azevedo, 2005). Similar expressions should be used for the  $F_k$  and  $G_k$  interface fluxes. For the construction of the first-order scheme, one must identify the “left” (or  $L$ ) state, as the properties of the  $i$ -th volume and the “right” (or  $R$ ) state as those of the  $m$ -th volume.

The evaluation of the split fluxes in the van Leer context can be summarized as follows:

$$\begin{aligned} M_x \geq 1 &\Rightarrow E_e^+ = E_e \text{ and } E_e^- = 0, \\ M_x \leq -1 &\Rightarrow E_e^+ = 0 \text{ and } E_e^- = E_e, \\ |M_x| < 1 &\Rightarrow E_e^\pm = \begin{cases} f^\pm \\ f^\pm [(\gamma - 1)u \pm 2a] / \gamma \\ f^\pm v \\ f^\pm w \\ f^\pm \left[ \frac{\{(\gamma - 1)u \pm 2a\}^2}{2(\gamma^2 - 1)} + \frac{v^2}{2} + \frac{w^2}{2} \right] \end{cases}. \end{aligned} \quad (8)$$

In the previous equations, the Mach number in the  $x$ -direction is defined as  $M_x = u/a$  and the split mass fluxes are  $f^\pm = \pm \rho a [(M_x \pm 1)/2]^2$ . Similar expressions are obtained for  $F^\pm$  using  $M_y = v/a$ , and for  $G^\pm$  using  $M_z = w/a$ . With this flux vector definition, the splitting is continuously differentiable at sonic and stagnation points.

## 4.3 First- and Second-Order Liou Schemes

The approach followed in the present work in order to extend Liou's ideas (Liou, 1994) to the unstructured grid case consists in defining a local one-dimensional stencil normal to the face considered. The Liou schemes implemented in this work consider that the flux vectors can be expressed as a sum of the convective and pressure terms (Liou, 1994, 1996). For the construction of the Liou schemes, one can assume that the convective operator may be written as

$$C(Q_i) = \sum_{k=1}^{nf} [E_k n_x + F_k n_y + G_k n_z] |\vec{S}_k| = \sum_{k=1}^{nf} \left[ (F_k^{(c)} + P_k) |\vec{S}_k| \right], \quad (9)$$

where  $F_k^{(c)}$  represents the contribution of the convective terms and  $P_k$  represents the pressure terms. Moreover,  $(n_x, n_y, n_z)$  are the components of the unit vector normal to the face and oriented outward with regard to the  $i$ -th control volume. In order to write the expressions of  $F_k^{(c)}$  and  $P_k$ , the inviscid flux vectors can be written as

$$E_e = u\Phi + P_x = M_x a \Phi + P_x, \quad F_e = v\Phi + P_y = M_y a \Phi + P_y, \quad G_e = w\Phi + P_z = M_z a \Phi + P_z, \quad (10)$$

where the  $\Phi$ ,  $P_x$ ,  $P_y$  and  $P_z$  vectors are defined as

$$\Phi = \begin{Bmatrix} \rho \\ \rho u \\ \rho v \\ \rho w \\ \rho H \end{Bmatrix}, \quad P_x = \begin{Bmatrix} 0 \\ p \\ 0 \\ 0 \\ 0 \end{Bmatrix}, \quad P_y = \begin{Bmatrix} 0 \\ 0 \\ p \\ 0 \\ 0 \end{Bmatrix}, \quad P_z = \begin{Bmatrix} 0 \\ 0 \\ 0 \\ p \\ 0 \end{Bmatrix}. \quad (11)$$

In the previous expressions,  $p$  is the pressure,  $H$  is the total specific enthalpy,  $M_x = u/a$ ,  $M_y = v/a$  and  $M_z = w/a$ . Hence, one could write that

$$F_k^{(c)} = [(un_x + vn_y + wn_z) \Phi]_k, \quad P_k = (n_x P_x + n_y P_y + n_z P_z)_k. \quad (12)$$

For the construction of the first-order scheme, one must identify the “left” (or  $L$ ) state, as defined in Liou (1994, 1996), as the properties of the  $i$ -th volume and the “right” (or  $R$ ) state as those of the  $m$ -th volume. The second-order scheme follows exactly the same formulation, except that the left and right states are obtained by a MUSCL extrapolation of primitive variables (Farney and Azevedo, 2005). The definition of the interface properties follows the standard formulation of the AUSM<sup>+</sup> scheme (Liou, 1996). Hence, the interface Mach number,  $M_k$ , can be written as

$$M_k = M_L^+ + M_R^- , \quad (13)$$

where  $M_L^+ = M^+(M_L)$  and  $M_R^- = M^-(M_R)$ . The split Mach numbers are defined as

$$M_L^+ = \begin{cases} \frac{1}{2} (M_L + |M_L|) & , \text{ if } |M_L| \geq 1, \\ M_\beta^+(M_L) & , \text{ otherwise,} \end{cases} , \quad M_R^- = \begin{cases} \frac{1}{2} (M_R - |M_R|) & , \text{ if } |M_R| \geq 1, \\ M_\beta^-(M_R) & , \text{ otherwise.} \end{cases} \quad (14)$$

The  $M_\beta^\pm$  terms can be written as

$$M_\beta^\pm(M) = \pm \frac{1}{4} (M \pm 1)^2 \pm \beta (M^2 - 1)^2 . \quad (15)$$

This work used  $\beta = 1/8$ , as suggested in Liou (1994). Moreover, in order to achieve a unique splitting in Liou’s sense, the left and right Mach numbers are defined as

$$M_L = \frac{\tilde{V}_L}{a_k} \quad \text{and} \quad M_R = \frac{\tilde{V}_R}{a_k} , \quad (16)$$

where

$$\begin{aligned} \tilde{V}_L &= u_L n_x + v_L n_y + w_L n_z , \\ \tilde{V}_R &= u_R n_x + v_R n_y + w_R n_z . \end{aligned} \quad (17)$$

The corresponding speed of sound,  $a_k$ , at the interface is given by

$$a_k = \min(\tilde{a}_L, \tilde{a}_R) , \quad \tilde{a}_L = a_L^* \cdot \min\left(1, \frac{a_L^*}{|\tilde{V}_L|}\right) , \quad a_L^* = \sqrt{\frac{2(\gamma-1)}{(\gamma+1)}} H_L , \quad (18)$$

and a similar definition for  $\tilde{a}_R$ . The pressure,  $p_k$ , at the  $k$ -th interface is given by

$$p_k = p_L^+ p_L + p_R^- p_R . \quad (19)$$

The split pressures, still following the expressions in Liou (1994), can be written as

$$p_L^+ = \begin{cases} \frac{1}{2} (1 + \text{sign}(M_L)) & , \text{ if } |M_L| \geq 1, \\ p_\alpha^+(M_L) & , \text{ otherwise,} \end{cases} , \quad p_R^- = \begin{cases} \frac{1}{2} (1 - \text{sign}(M_R)) & , \text{ if } |M_R| \geq 1, \\ p_\alpha^-(M_R) & , \text{ otherwise.} \end{cases} \quad (20)$$

The  $p_\alpha^\pm$  terms can be written as

$$p_\alpha^\pm(M) = \frac{1}{4} (M \pm 1)^2 (2 \mp M) \pm \alpha M (M^2 - 1)^2 . \quad (21)$$

This work used  $\alpha = 3/16$ , as suggested in Liou (1994). Therefore, with the interface properties so defined and using Eq. (12), the  $F_k^{(c)}$  and  $P_k$  vectors can be finally written as

$$F_k^{(c)} = \frac{1}{2} M_k a_k (\Phi_L + \Phi_R) - \frac{1}{2} |M_k| a_k (\Phi_R - \Phi_L) , \quad (22)$$

and

$$P_k = \begin{Bmatrix} 0 \\ pn_x \\ pn_y \\ pn_z \\ 0 \end{Bmatrix} . \quad (23)$$

Hence, the convective operator,  $C(Q_i)$ , can be computed using Eq. (9).

## 5. Results and Discussion

A 3-D inlet configuration which is representative of some proposed inlet geometries for a typical transatmospheric vehicle was used as a test in the present work (Heidi, 1998). For the present simulations, the fluid was treated as a perfect gas with constant specific heat and no chemistry was taken into account. The purpose of these simulations is to compare the different schemes applied to high Mach number flows in order to verify if they are able to represent all flow features, such as strong shocks, shock reflections and interactions, and expansion regions. Moreover, there is interest in verifying whether the schemes can avoid oscillations in the presence of such strong discontinuities.

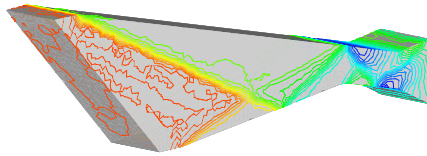
The results considering inlet entrance Mach numbers from  $M_\infty = 4$  up to  $M_\infty = 12$  are discussed in the paper. The initial grid had 58174 tetrahedral volumes. This mesh ended up with 123983 volumes after the refinement procedure. In Figs. 1(a)–1(e) one can observe the Mach number contours obtained with the refined mesh. In these test cases, the problem considers the internal flow in the inlet configuration with entrance Mach number  $M_\infty = 4$ . For all simulations, a constant  $CFL = 0.2$  is used. The figures present, respectively, the results with a 2nd-order central difference-type scheme, the 1st- and 2nd-order van Leer flux-vector splitting schemes and the 1st- and 2nd-order Liou AUSM<sup>+</sup> schemes. The contours indicate that the overall flow features are well captured by all solutions. The contours for both upper and lower wall entrance shocks for all upwind schemes calculations are an indication that there are no oscillations in these solutions. However, in the centered scheme, one can observe some oscillations in the upstream portion of the flow. The quantitative results, in terms of pressure coefficient distributions along the upper and lower entrance ramp with the 2nd-order centered scheme, the 1st- and 2nd-order van Leer schemes, and the 1st- and 2nd-order Liou schemes are shown in Figs. 2(a) to 2(f). The available analytical solutions, which are valid upstream of the shock interactions, are compared with the numerical results obtained with the present numerical tool. One can observe that the upper wall shock and the lower wall shock are less oscillatory in the computations with the 1st-order van Leer upwind scheme. This is to be expected since this scheme is quite a bit more diffusive than the other schemes tested in the paper.

The shock positions have been fairly well captured for all test cases presented in this paper, although there is clearly some smearing of the shocks, as one can see in Figs 2(a) to 2(f). It is also correct to state that the results for the upper wall shock seem to be slightly better resolved than those for the lower wall. In general, good qualitative results are obtained with the present numerical tool. The more diffusive character of 1st-order schemes is evident in the quantitative results presented. Pressure coefficient distributions calculated indicate that the additional numerical diffusivity of 1st-order schemes can destroy some of the information in the downstream regions. Moreover, it is also clear that the upper wall entrance shock is more sharply defined by the 2nd-order upwind solutions than by the 1st-order upwind calculations. It is important to emphasize that, for higher Mach numbers, the upper wall entrance shock is more sharply defined by the upwind solutions than by the calculations obtained with the centered scheme.

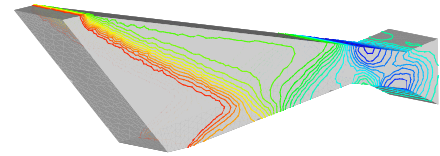
## 6. Concluding Remarks

The present work intends to perform a comparison of five different spatial discretizations schemes for cold gas hypersonic flow simulations. The schemes here presented are applied to the solution of supersonic and hypersonic inlet flows. The inlet entrance conditions are varied from  $M_\infty = 4$  up to  $M_\infty = 12$ . A viscous formulation is available in the code, but the results included in the present paper only considered inviscid computations, and the fluid was treated as a perfect gas. In actual flight, an inlet flow with an entrance Mach number equal to 12 could not be simulated with the perfect gas assumption. In other words, real gas behavior would have to be taken into account. From a physical standpoint, however, the present calculations could be considered as the simulation of the cold gas flows which are usually achieved in experimental facilities such as gun tunnels. In order to extrapolate these results to actual flight conditions, dissociation and vibrational relaxation would certainly have to be included in the formulation. Nevertheless, the present simulations could be seen as a necessary step in the construction of a robust code to deal with the complete environment encountered in actual flight. Here, however, the consideration of very high Mach number flows has simply the objective of testing the behavior of the different schemes in the presence of strong shocks.

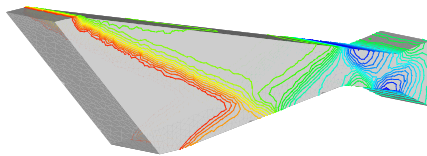
The equations are advanced in time by an explicit, 5-stage, 2nd-order accurate, Runge-Kutta time stepping procedure. The spatial discretization considers a centered scheme and two upwind schemes, namely van Leer and Liou flux-vector splitting schemes, with both 1st- and 2nd-order implementations. The implementation of the 2nd-order versions of the two upwind schemes uses MUSCL reconstruction in order to obtain left and right states at interfaces. The 1st-order van Leer flux vector splitting scheme has reduced the flow property oscillations. However, as one could expect, this 1st-order method also causes considerable smearing of the flow discontinuities due to the excessive artificial dissipation intrinsically added. In a general manner, numerical solutions of complicated flows such as the supersonic and hypersonic inlet flows can be obtained in half the time used by the single-grid simulation.



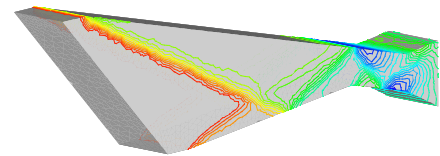
(a) 2nd-order centered scheme.



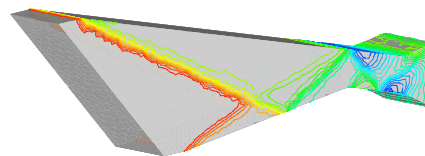
(b) 1st-order van Leer scheme.



(c) 2nd-order van Leer scheme.



(d) 1st-order Liou scheme



(e) 2nd-order Liou scheme

Figura 1. Mach number contours obtained for the five schemes implemented ( $M_\infty = 4$ ).

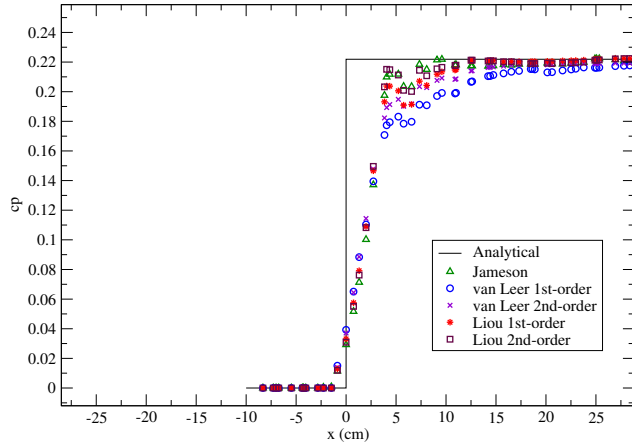
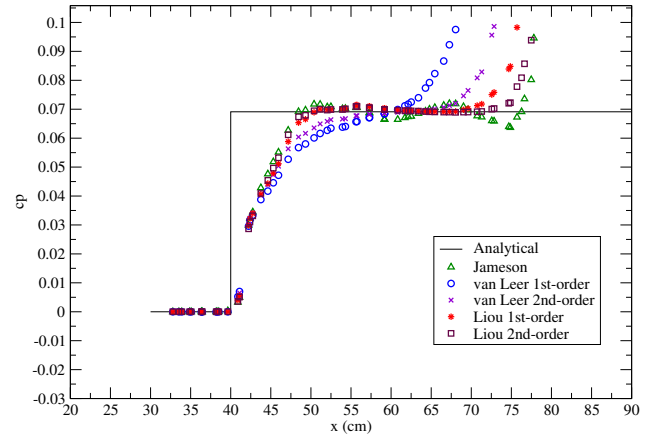
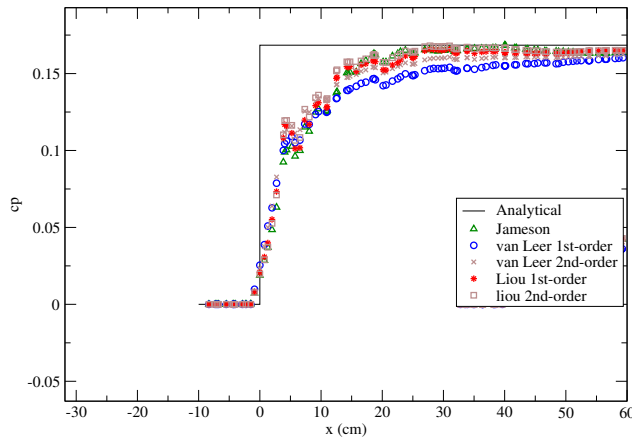
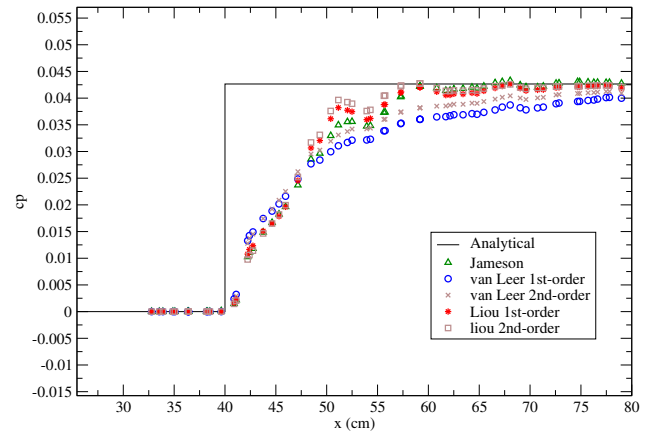
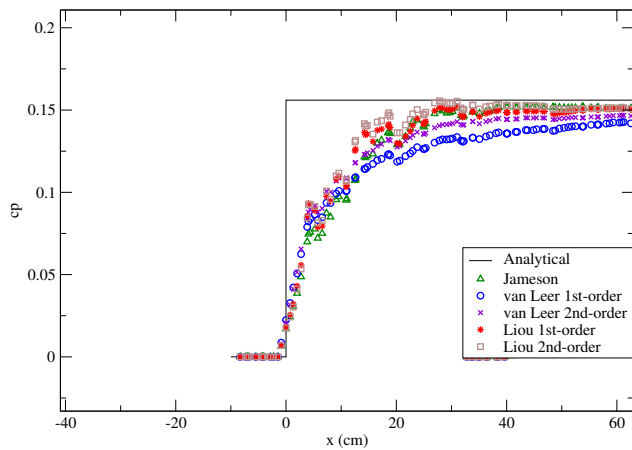
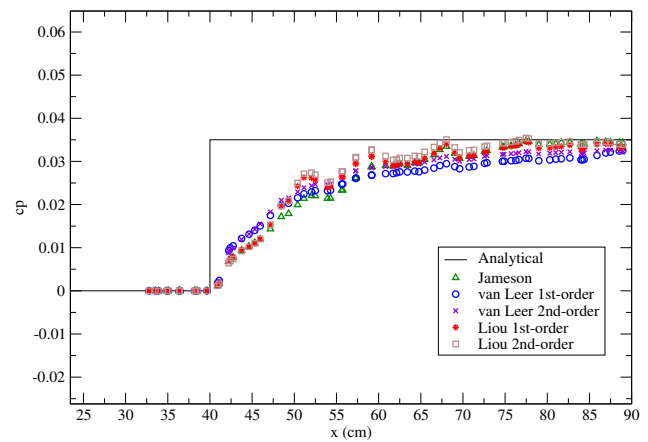
(a) Upper wall,  $M_\infty = 4$ .(b) Lower wall,  $M_\infty = 4$ .(c) Upper wall,  $M_\infty = 8$ .(d) Lower wall,  $M_\infty = 8$ .(e) Upper wall,  $M_\infty = 12$ .(f) Lower wall,  $M_\infty = 12$ .

Figure 2. Pressure coefficient distributions in the lower and upper walls for  $M_\infty = 4$  up to  $M_\infty = 12$ .

## 7. Acknowledgments

The authors gratefully acknowledge the support of Fundação de Amparo à Pesquisa do Estado de São Paulo, FAPESP, through a M.S. Scholarship for the first author under the FAPESP Grant No. 03/10209-2. The authors also acknowledge the partial support of Conselho Nacional de Desenvolvimento Científico e Tecnológico, CNPq, under the Integrated Project Research Grant No. 501200/2003-7.

## 8. References

- Steger, J. L. and Warming, R. F., "Flux Vector Splitting of the Inviscid Gasdynamic Equations with Application to Finite-Difference Methods," *Journal of Computational Physics*, Vol. 40, No. 2, Apr. 1981, pp. 263-293.
- van Leer, B., "Flux-Vector Splitting for the Euler Equations," *Proceeding of the 8th International Conference on Numerical Methods in Fluid Dynamics, Lecture Notes in Physics*, Vol. 170, Springer-Verlag, Berlin, 1982, pp. 507-512.
- Liou, M.-S., "A Sequel to AUSM: AUSM<sup>+</sup>," *Journal of Computational Physics*, Vol. 129, No. 2, 1996, pp. 364-382.
- Anderson, W. K. and Thomas, J. L. and van Leer, B., "A Comparison of Finite Volume Flux Vector Splittings for the Euler Equations," *AIAA Journal*, Vol. 24, No. 9, Sept. 1986, pp. 1453-460.
- Pulliam, T. H. and Steger, J. L., "Implicit Finite-Difference Simulations of Three-Dimensional Compressible Flow," *AIAA Journal*, Vol. 18, No. 2, Feb. 1980, pp. 159-167.
- Moreira, Farney C. and Azevedo, J. L. F., "A Study of Spatial Discretization Schemes Applied to Cold Gas Hypersonic Flow Simulations," AIAA Paper, *Applied Aerodynamics Conference*, Toronto, CA, June 2005.
- Korzenowski, H. and Figueira da Silva, L. F. and Azevedo, J. L. F., "Unstructured Adaptive Grid Flow Simulations of Inert and Reactive Gas Mixtures," *Proceedings of the 14th Brazilian Congress of Mechanical Engineering - COBEM 97*, Bauru, SP, Brazil, Dec. 1997.
- Jameson, A. and Schmidt, W. and Turkel, E., "Numerical Solution of the Euler Equations by Finite Volume Methods Using Runge-Kutta Time-Stepping Schemes," AIAA Paper 81-1259, *14th AIAA Fluid and Plasma Dynamics Conference*, Palo Alto, CA, June 1981.
- Azevedo, J. L. F. and Figueira da Silva, L. F., "The Development of an Unstructured Grid Solver for Reactive Compressible Flow Applications," AIAA Paper 97-3239, *33rd AIAA/ASME/SAE/ASEE Joint Propulsion Conference & Exhibit*, Seattle, WA, July 1997.
- van Leer, B., "Towards the Ultimate Conservative Difference Scheme. V. A Second-Order Sequel to Godunov's Method," *Journal of Computational Physics*, Vol. 32, No. 1, July 1981, pp. 101-136.
- Hirsch, C., "Numerical Computation of Internal and External Flows," *Computational Methods for Inviscid and Viscous Flows*, Vol. 2, Wiley, New York, 1st ed., 1990, pp. 408-443.
- Liou, M.-S., "A Continuing Search for a Near-Perfect Numerical Flux Scheme. Part I: AUSM<sup>+</sup>," NASA TM-106524, Mar. 1994.